Evaluating Adversarial Evasion Attacks in the Context of Wireless Communications

Bryse Flowers, R. Michael Buehrer, and William C. Headley

Abstract—**Recent advancements in radio frequency machine learning (RFML) have demonstrated the use of raw in-phase and quadrature (IQ) samples for multiple spectrum sensing tasks. Yet, deep learning techniques have been shown, in other applications, to be vulnerable to adversarial machine learning (ML) techniques, which seek to craft small perturbations that are added to the input to cause a misclassification. The current work differentiates the threats that adversarial ML poses to RFML systems based on where the attack is executed from: direct access to classifier input, synchronously transmitted over the air (OTA), or asynchronously transmitted from a separate device. Additionally, the current work develops a methodology for evaluating adversarial success in the context of wireless communications, where the primary metric of interest is bit error rate and not human perception, as is the case in image recognition. The methodology is demonstrated using the well known Fast Gradient Sign Method to evaluate the vulnerabilities of raw IQ based Automatic Modulation Classification and concludes RFML is vulnerable to adversarial examples, even in OTA attacks. However, RFML domain specific receiver effects, which would be encountered in an OTA attack, can present significant impairments to adversarial evasion.**

Index Terms—**cognitive radio security, machine learning, modulation classification**

I. INTRODUCTION

The advent of deep learning has changed the face of many fields of research in recent years, including the wireless communications domain. In particular, Radio Frequency Machine Learning (RFML), a research thrust championed by DARPA that seeks to develop RF systems that learn from raw data rather than hand-engineered features, has garnered the interest of many researchers. One subset of RFML deals with utilizing raw in-phase and quadrature (IQ) samples for spectrum sensing. Spectrum sensing can be used in Dynamic Spectrum Access (DSA) systems to determine the presence of primary and secondary users in order to adapt transmission parameters to the environment [1] and has obvious applications to signals intelligence. Prior approaches to spectrum sensing were likelihood or feature based [2]–[7] while more recent approaches leverage the advances in deep neural networks (DNN) to operate directly on raw IQ samples [8]–[13].

While the popularity of RFML has increased, the study of the vulnerabilities of these systems to adversarial machine learning [14] has lagged behind. Adversarial machine learning

consists of learning to apply small perturbations to input examples that cause a misclassification. The increased activity in deep learning research in wireless is sure to draw the attention of attackers in this domain but is just beginning to be researched [15], [16]. Adversarial machine learning could be used, in the context of RFML, to disrupt DSA systems through primary user emulation [17], evade mobile transmitter tracking [18], or avoid demodulation by confusing an Automatic Modulation Classification (AMC) system [2].

While research thrusts towards adversarial machine learning evasion attacks and defenses can build off of the large body of literature present in the Computer Vision (CV) domain, RFML has additional adversarial goals and capabilities beyond those typically considered in CV. Adversarial goals must be split between attacks that have direct access to the classifier input, those that originate from the transmitter and therefore propagate synchronously with the underlying transmission through a stochastic channel, and those that originate asynchronously from a separate transmitter and are only combined at the receiver or eavesdropper. Additionally, in the context of wireless communications, attacks must be characterized against the primary metric of interest, bit error rate (BER). An adversary may seek to evade an eavesdropping classifier but that is of limited benefit if it also corrupts the transmission to a cooperative receiver.

The current work consolidates the additional adversarial goals and capabilities present in RFML and proposes a new threat model. Using the well known Fast Gradient Sign Method (FGSM) [19], results are presented from multiple example attacks against raw-IQ based AMC in order to draw general conclusions about the current vulnerabilities of RFML systems to adversarial machine learning attacks that have direct access to the AMC input as well as attacks that occur over the air (OTA). The current work is organized as follows: Section II surveys the related work in this area, Section III presents a consolidated threat model for RFML systems, Section IV describes the methodology for executing and evaluating the adversarial evasion attacks in the context of wireless communications, Section V and VI analyze the attack's effectiveness with direct access to the classifier input and in an OTA environment respectively, and conclusions are presented in Section VII.

II. RELATED WORK

Threats to machine learning have a wide span in the literature. Causative attacks exert influence over the training process to inject vulnerabilities into the trained classifier [21], [22].
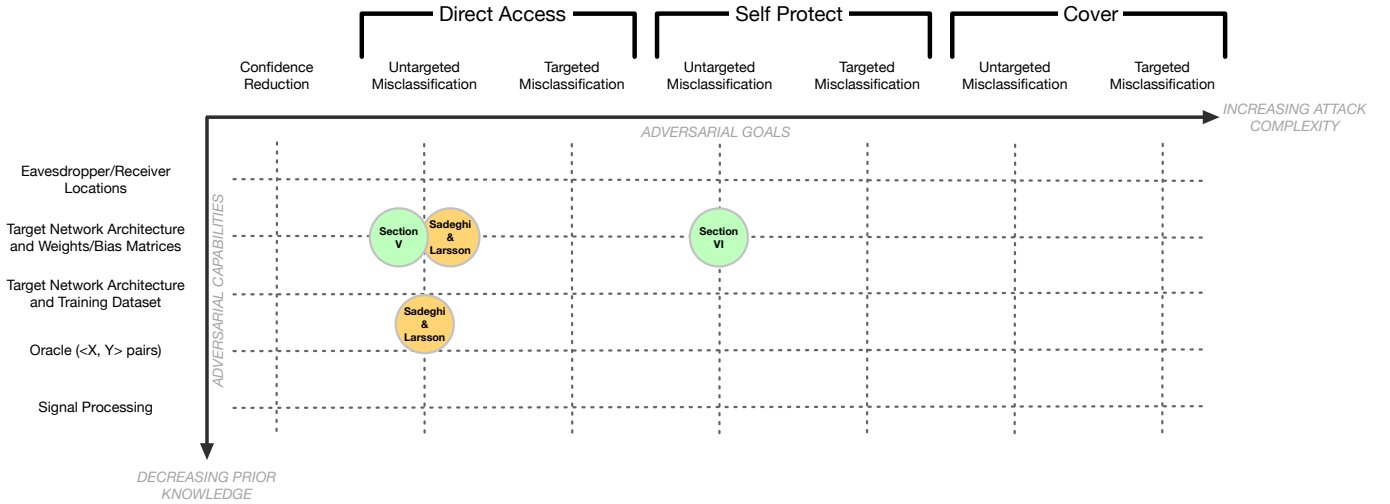
Fig. 1. Threat Model for RFML signal classification systems presented in the style of [20]. The current work presents results for untargeted misclassification in both a direct access and self protect scenario with full knowledge of the target network architecture and learned parameters. The related work by Sadeghi and Larsson [15] presented an analysis of two untargeted misclassification attacks against AMC without a channel model applied to the perturbations. One attack assumed perfect knowledge of the target network and the other only assumed knowledge of the entire training dataset.

Exploratory attacks [14] seek to learn information about the classifier. The current work is primarily concerned with evasion attacks [23]–[25] which seek to cause a misclassification at inference time. Specifically, this work uses the well known FGSM attack, first proposed in [19] for a CV application, as the algorithm for crafting adversarial perturbations due to its low computational complexity; however, the methodology for evaluating the attack effectiveness will hold for all current evasion attacks.

Prior security threats to cognitive signal classifiers have been researched [26], [27], yet, the state of the art signal classification systems use deep learning techniques [8]–[13] whose vulnerabilities have not been studied extensively in the context of RF. In [16] and [28], the authors consider adversarial machine learning for intelligently jamming a deep learning enabled transmitter, at transmission time and sensing time, to prevent a transmission. Their work considers learning OTA by observing an acknowledgement from a receiver as a binary feedback. While their work is primarily concerned with preventing transmission, the current work is primarily concerned with enabling transmission while avoiding eavesdroppers and is thus fundamentally different.

The work presented in [15] is the closest analogy to the current work. The authors present a study of a similar neural network architecture [8] using the RML2016.10A dataset [29]. The authors present results from attacks on this DNN using modifications of FGSM [19] and Universal Adversarial Perturbations (UAP) [23]. Using their adaptation of UAP, they are able to show black-box[1] results which are time shift invariant, which is a limitation of FGSM. Additionally, the authors use the energy ratios of the perturbation and modulated signal as an attack constraint, a metric that the current work uses as well. However, the authors consider perturbations which are below the noise floor but implicitly assume they are able to

compromise the eavesdropper's signal processing chain by not considering the effect of the channel on the perturbation signal. Therefore, [15] only considers attacks that have direct-access to the classifier and aren't transmitted OTA. The current work expands upon the study of white-box[2] direct-access attacks against RFML systems by exploring the vulnerabilities versus neural network input size. Additionally, the current work considers white-box self-protect attacks, which are launched OTA, where receiver effects can negatively impact adversarial success and must also be evaluated against the effect the perturbation has on the underlying signal transmission by characterizing the BER.

III. THREAT MODEL FOR RFML

A rich taxonomy already exists for describing threat models for adversarial machine learning in the context of CV; however, threat models which only consider CV applications lack adversarial goals and capabilities that are unique to RFML. Therefore, the current work extends the threat model initially proposed in [20] for RFML in Figure 1. This section first describes the system model considered for AMC and then expands on the unique categories of adversarial goals and capabilities that must be considered when discussing adversarial threats to RFML systems.

A. Automatic Modulation Classification System Model

The current work considers the task of blind signal classification where an eavesdropper attempts to detect a signal in the spectrum, isolate it in time and frequency, and perform modulation classification. This task assumes that the signal is a wireless communication between a transmitter and a cooperative receiver where the eavesdropper is not synchronized and has very limited *a priori* information about

---

[1]Black-box refers to attacks with full access to the training dataset but no knowledge of the DNN architecture of learned parameter matrices.

[2]White-box refers to attacks with perfect knowledge of the learned parameter matrices of the DNN.

the communication. Ultimately, the eavesdropper could then use the output for DSA, signals intelligence, and/or as a preliminary step to demodulating the signal and extracting the actual information transmitted.

The study of adversarial examples in this model could be framed from the perspective of either the eavesdropper or the transmitter. First, this study can be considered a vulnerability analysis of RFML systems and the information gained can then be used to produce a more robust eavesdropper that is hardened against deception by adversarial machine learning. Additionally, this study could be considered a feasibility analysis for methodology to protect transmissions from eavesdroppers. Evading an eavesdropper can limit tracking of the transmitter or automatic demodulation of its transmission. The current work does not take a side in the application of this technology and presents a case for both sides; however, the term adversary is used to describe the transmitter that seeks to evade an eavesdropper for the remainder of the current work.

B. Adversarial Goals

Three main goals are traditionally considered for adversarial machine learning [20]: confidence reduction, untargeted misclassification, and targeted misclassification. Confidence reduction is the easiest goal an adversary can have. It simply refers to introducing uncertainty into the classifier's decision even if it ultimately determines the class of signal correctly. An adversary whose goal is simply to be classified as any other signal type than its true class, can be described as untargeted misclassification. Targeted misclassification is typically the most difficult goal of adversarial machine learning. It occurs when an adversary desires a classifier to output a specific target class instead of simply any class that is not the true class. Due to the hierarchical nature of human engineered modulations, the difficulty of targeted misclassification for AMC depends heavily on the signal formats of the true and target class. Targeted misclassification are sometimes split between attacks that start with a real input [19], [25] versus those that start with noise [30]. The threat model presented in Figure 1 only considers the former because the current work assumes that an adversary's primary goal is to transmit information and not simply degrade classifier performance.

Further, the current work categorizes adversarial goals based on where the attack is launched from.

1) Direct Access: Traditional adversarial machine learning, such as those generally considered in CV or the attack considered in [15], fall into the direct access category. This category of attack is performed "at the eavesdropper" as part of their signal processing chain. Therefore, the propagation channel and receiver effects for the example is known at the time of crafting the perturbation, the perturbation is not subjected to any receiver effects, and the perturbation will have no effect on the intended receiver because it is not sent OTA. Attacks at this level are very useful for characterizing the worst case vulnerabilities of a classifier but they are less realistic in the context of RFML because it assumes that the signal processing chain has been compromised.

2) Self Protect: When the adversarial perturbation is added at the transmitter and propagates along with the transmitted signal to the eavesdropper, this can be categorized as self protect. By adding the perturbation at the transmitter, the perturbation can still be completely synchronous with the signal transmission; however, the perturbation will now be subjected to all of the receiver effects traditionally considered in RFML and will also impact the intended receiver. While many of the algorithms that are successful for the direct access category of attacks will be applicable to self protect, the evaluation of adversarial success must take into account receiver effects. Therefore, attacks that seek to create minimal perturbations, such as the modified FGSM method presented in [15], will no longer work because adversarial success can not be guaranteed due to the signal being subjected to a stochastic process.

3) Cover: RFML allows for a third category of adversarial goals, in which the adversarial perturbation originates from a separate emitter from the transmitter and is only combined at the eavesdropping device. Low cost transmitters can be size, weight, and power (SWaP) constrained. Therefore, it may be beneficial to have a single unit provide cover for multiple SWaP constrained nodes. However, because these attacks cannot rely on synchronization between the transmission and perturbation, the perturbations must be time shift invariant [15] making this category of attack more difficult. The current work does not present a study of this category of adversarial goal and leaves that to future work.

C. Adversarial Capabilities

Traditional adversarial machine learning capabilities, such as those described in [20], generally help with determining "what you want a classifier to see" by providing information about the target DNN that can subsequently be used to optimize the input. In the most extreme case, attacks may have perfect knowledge of the learned parameters of the model. These attacks are referred to as white-box. In a slightly more realistic case, the attacker may have access to the network architecture and training dataset, but not the learned parameters. The attacker must then create adversarial examples that generalize over all possible models created from the dataset and architecture. In a very limited case, the attacker may only have access to what is deemed an oracle, an entity that will label a limited number of X, Y pairs for the attacker through an API [31] or an observable wireless transmission [16], [28]. This allows the attacker to perform limited probes against the target network in order to build up an attack.

Adversarial machine learning applied to RFML has a different class of capabilities an attacker can possess that can be thought of as "the ability to make a classifier see a specific example". RF propagation can be directed through the use of smart antennas. Therefore, if a transmitter knew the location of the receiver, it could direct its energy only at the receiver, thus minimizing the signal-to-noise ratio (SNR) at the eavesdropper. Similarly, a jammer could direct energy only at the eavesdropper, maximizing the impact of perturbations on classification accuracy while minimizing the impact to the receiver.
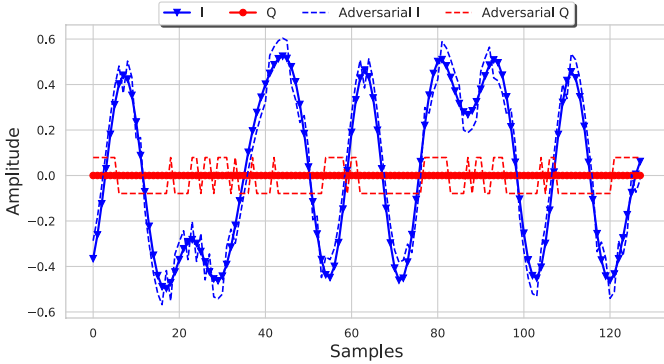
Fig. 2. BPSK adversarial example with a 10 dB (E_s/E_j) perturbation, created with the FGSM [19] algorithm, applied.

Signal processing chains can present an impediment to adversarial success. Traditionally, RF front ends are built to reject out of band interference and therefore adversarial perturbations consisting of high frequencies could be filtered out. Power amplifiers can exhibit non-linear characteristics which would distort the perturbation. Further, the precision of the analog to digital converter could limit the attack to stair stepped ranges.

D. Threat Model Assumed in the Current Work

In the current work we assume direct access to the learned parameters of the target DNN and set the goal as untargeted misclassification. The current work considers perturbations that are specific to the underlying transmitted signal and characterizes their effectiveness in the presence of receiver effects such as noise, sample time offsets, and frequency offsets. Therefore, both direct access attacks as well as self protect are considered. The current work does not assume knowledge of either the eavesdropper or receiver locations and therefore does not consider directional antennas and instead shows results across varying SNR ranges. Further, the current work assumes that the receiver is fixed and thus does not introduce any modifications to the receive chain.

IV. METHODOLOGY

Most raw-IQ based signal classifiers seek to take in a signal snapshot, x, and output the most probable class y. Traditionally, x would represent a single channel of complex samples, with little pre-processing performed, and could therefore be represented as a two-dimensional matrix [IQ, number of samples]. Specifically, RFML systems, which generally use DNNs, learn a mapping from the data by solving

$$\operatorname*{argmin}_{\boldsymbol{\theta}} \mathcal{L}(f(\boldsymbol{\theta}, \boldsymbol{x}), \boldsymbol{y})), \tag{1}$$

where x and y represent the training inputs and target labels respectively and f represents the chosen network architecture. A loss function ($\mathcal{L}$), such as categorical cross entropy, is generally used in conjunction with an optimizer, such as stochastic gradient descent or Adam [32], to train the DNN and thus learn the network parameters $\boldsymbol{\theta}$. While training the

model, the dataset is fixed (assuming no data augmentation) and is assumed to be sampled from the same distribution that will be seen during operation of the RFML system.

Untargeted adversarial machine learning is simply the inverse of this process. By seeking to maximize the same loss function, an adversary can decrease the accuracy of a system. Therefore, the adversary is also solving an optimization problem that can be defined by the following.

$$\operatorname*{argmax}_{\boldsymbol{x}^*} \mathcal{L}(f(\boldsymbol{\theta}, \boldsymbol{x}^*), \boldsymbol{y})) \tag{2}$$

In this case, the parameters, $\boldsymbol{\theta}$, of the classifier are fixed but the input, $\boldsymbol{x}^*$, can be manipulated. Many approaches exist to solve this problem. In particular, FGSM [19] creates untargeted adversarial examples using

$$\boldsymbol{x}^* = \boldsymbol{x} + \epsilon \times \operatorname{sign}(\nabla_x \mathcal{L}(f(\boldsymbol{\theta}, \boldsymbol{x}), \boldsymbol{y})), \tag{3}$$

where y represents the true input label and ∇_x represents the gradient of the loss function with respect to the original input, x. This methodology creates adversarial examples constrained by a distance, ϵ, in the feature space in a single step. $\boldsymbol{x}^*$ is referred to as an adversarial example. One adversarial example used in the current work is presented in Figure 2, where the source modulation is BPSK and a perturbation has been applied to achieve untargeted evasion for a direct access attack.

In the context of wireless communications, the absolute value of the signal is generally less important than the relative power of the signal with respect to some other signal such as noise. Therefore, similar to [15], the current work reformulates the perturbation constraint, ϵ, from a distance bounding in the feature space to a bounding of power ratios. Additionally, the signal can be directly evaluated on the primary metric of interest, BER, as opposed to the use of human perception, or a proxy for it such as ϵ, in CV. Further,

A. Adapting FGSM

The average energy per symbol (E_s) of a transmission can be computed using

$$\mathbb{E}[E_s] = \frac{\text{sps}}{N} \sum_{i=0}^{N} |s_i|^2, \tag{4}$$

where sps represents samples per symbol, N is the total number of samples, and s_i represents a particular sample in time. Without loss of generality, the current work assumes the average energy per symbol of the modulated signal, E_s, is 1. Therefore, the power ratio of the underlying transmission to the jamming/perturbation signal[3] (E_j) can be derived as

$$\begin{aligned} \frac{E_s}{E_j} &= \frac{1}{E_j} \\ &= 10^{-E_j(\text{dB})/10} \end{aligned} \tag{5}$$

---

[3]Because the perturbation is an electronic signal deliberately crafted to impair the successful operation of the eavesdropper, the current work uses jamming signal and perturbation signal interchangeably.
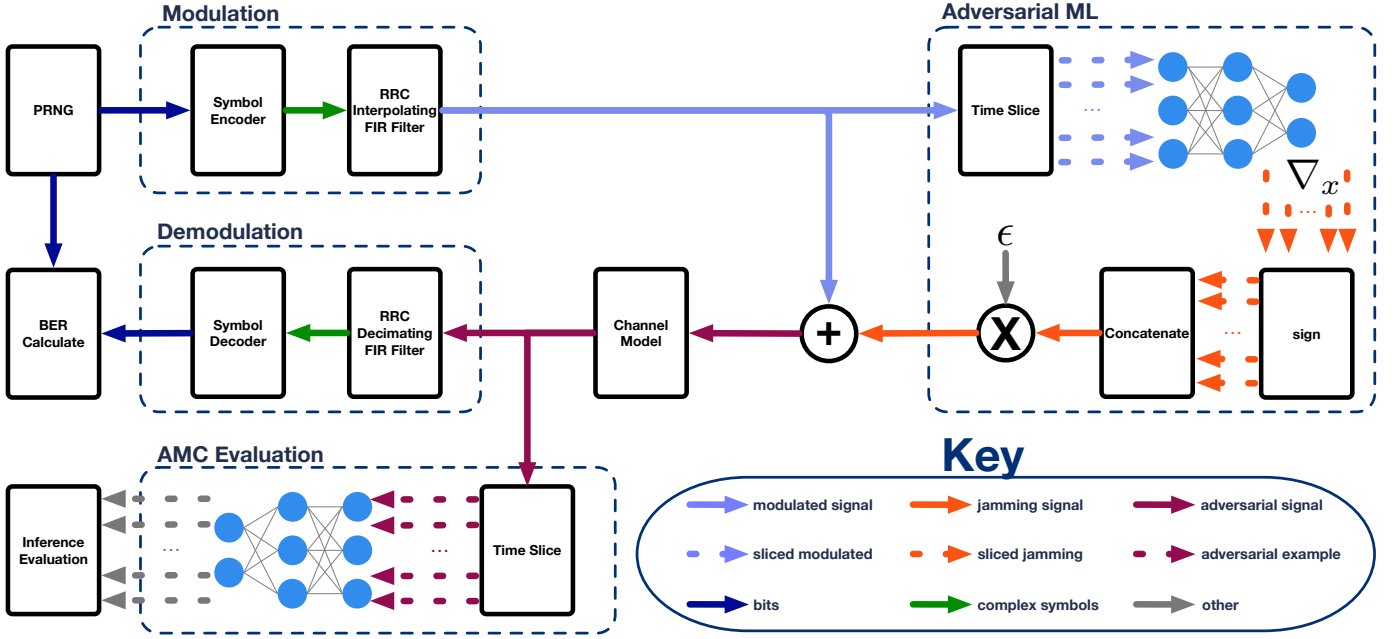
Fig. 3. Block diagram of the evaluation methodology developed for the current work. The current work assumes perfect knowledge of the target DNN and therefore the DNN shown in the AMC Evaluation and Adversarial ML blocks are identical and simply separated for clarity.

Since the input of $\text{sign}(\nabla_x)$ in (3) is complex, the output is also complex, and is therefore a vector whose values are $(\pm 1, \pm 1 j)$. Therefore, the magnitude of each sample of the jamming signal can be computed as

$$\begin{aligned} |\text{sign}(\nabla_x)| = |\text{sign}(z)| \\ = \sqrt{(\pm 1)^2 + (\pm 1)^2} \\ = \sqrt{2} \end{aligned} \tag{6}$$

Thus the energy per symbol of $\text{sign}(\nabla_x)$ can be computed by plugging (6) into (4) resulting in

$$\begin{aligned} E_{\text{sign}(\nabla_x)} = \frac{\text{sps}}{N} \sum_{i=0}^{N} |\text{sign}(\nabla_x)|^2 \\ = 2 \times \text{sps} \end{aligned} \tag{7}$$

Because sps is fixed throughout transmission, a closed form scaling factor, ϵ, can be derived to achieve the desired energy ratio (E_s/E_j) by using

$$\begin{aligned} \epsilon = \sqrt{\frac{\frac{E_s}{E_j}}{E_{\text{sign}(\nabla_x)}}} \\ = \sqrt{\frac{10^{\frac{-E_j}{10}}}{2 \times \text{sps}}} \end{aligned} \tag{8}$$

Plugging ϵ into (3) allows the creation of adversarial examples constrained by E_s/E_j and can be succinctly defined as

$$\boldsymbol{x}^* = \boldsymbol{x} + \sqrt{\frac{10^{\frac{-E_j}{10}}}{2 \times \text{sps}}} \times \text{sign}(\nabla_x \mathcal{L}(f(\boldsymbol{\theta}, \boldsymbol{x}), \boldsymbol{y})) \tag{9}$$

Constraining the power ratio in this way can be useful for evaluating system design trade-offs. Any given transmitter has a fixed power budget and the current work considers an adversarial machine learning technique which is not aware of the underlying signal; therefore, power which is used for the jamming signal subsequently cannot be used for the underlying transmission. Future adversarial machine learning techniques could take into account the bit error rate in their methodology which would allow for this energy to accomplish both purposes, but, this exploration is left to future work.

B. Simulation Environment

The high level overview of the simulation environment used in the current work is shown in Figure 3 and each major block is described below. Full evaluation in the context of wireless communications requires the interfacing of both a DSP and ML framework. The current work uses GNU Radio and PyTorch respectively; however, the methodology is not dependent upon use of those frameworks in any way.

1) Modulation: The initial modulated signal is generated by a simple flow graph in GNU Radio. Unless otherwise stated, the parameters for transmission can be summarized as follows. The symbol constellations used are BPSK, QPSK, 8PSK, and QAM16. The root raised cosine filter interpolates to 8 samples per symbol using a filter span of 8 symbols and a roll-off factor of 0.35. 1000 examples per modulation scheme are created using a random bit stream.

2) Adversarial ML: In order to craft the jamming signal using adversarial machine learning techniques it is necessary to first slice the signal into discrete examples matching the DNN input size. Before feeding these examples into the DNN, dithering is employed to add small amounts of noise to the examples. The FGSM algorithm is then used to create the

perturbations which are concatenated back together to form the jamming signal. For each E_s/E_j studied, the jamming signal is scaled linearly using (8) and added to the modulated signal. Unless otherwise stated, E_s/E_j is swept from 0 to 20 dB with a step size of 4 dB.

3) Channel Model: The current work considers a simple channel model with Additive White Gaussian Noise (AWGN) and center frequency offsets. The received signal can be characterized as follows:

$$S_{\text{rx}}(t) = e^{-j2\pi f_o t} S_{\text{tx}}(t) + \mathcal{N}(0, \sigma^2) \qquad (10)$$

Where f_o is the normalized frequency offset and σ^2 is given by the desired E_s/N_0. The channel model is again implemented using a GNU Radio flow graph.

4) Demodulation: Demodulating the received signal consists of match filtering, down-sampling to one sample per symbol, and decoding the symbols back into a bit stream to verify the data received matches the data transmitted. The demodulation is also implemented as a GNU Radio flow graph and assumes both symbol and frame synchronization.

5) Automatic Modulation Classification Evaluation: Top-1 accuracy is the metric used for classifier evaluation in [8], [9], and [33] and is the metric we use for evaluation in the current work. For untargeted adversarial machine learning, adversarial success is defined as a lower Top-1 accuracy as opposed to a higher accuracy.

C. Automatic Modulation Classification Target Network

1) Network Architecture: The current work uses the DNN architecture first introduced in [8] for raw-IQ modulation classification. This architecture consists of two convolutional layers followed by two fully connected layers. This network takes the IQ samples as a $[1, 2, N]$ tensor which corresponds to 1 channel, IQ, and N input samples. The current work uses extended filter sizes as done in [9] and [33], using filters with 7 taps and padded with 3 zeros on either side. The first convolutional layer has 256 channels, or kernels, and filters I and Q separately. The first layer does not use a bias term as this led to vanishing gradients during our training. The second layer consists of 80 channels and filters the I and Q samples together using a two-dimensional real convolution. This layer includes a bias term. The feature maps are then flattened and fed into two fully connected layers, the first consisting of 256 neurons and the second consisting of the number of output classes. All layers use ReLU as the activation function (except for the output layer). As a pre-processing step, the average power of each input is normalized to 1.

2) Dataset A: The majority of this work uses the open source RML2016.10A dataset introduced in [29]. This synthetic dataset consists of 11 modulation types: BPSK, QPSK, 8PSK, CPFSK, GFSK, PAM4, QAM16, QAM64, AM-SSB, AM-DSB, and WBFM. These signals are created inside of GNU Radio and passed through a dynamic channel model to create sample signals at SNRs ranging from -20dB to 18dB.

Using an open source dataset allows for quick comparison of results to those seen in literature; however, this dataset only provides one input size, 128 complex samples. Furthermore,
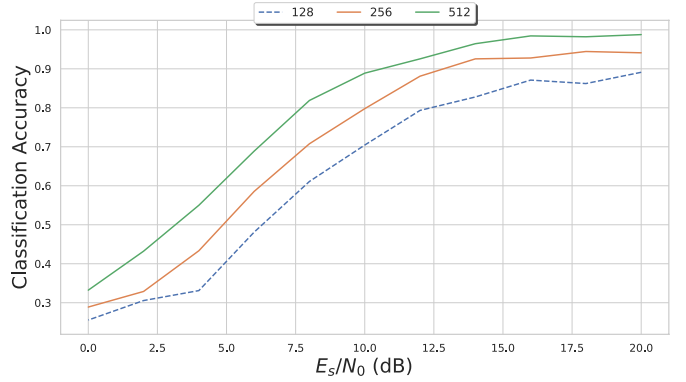

Fig. 4. Dataset B test accuracy vs SNR for three different neural network input sizes. As expected, increasing the input size results in increasing test accuracy over the entire SNR range studied.

this dataset contains limited center frequency offsets. Therefore, it was necessary to create an additional dataset to perform all of the evaluations contained in the current work.

3) Dataset B: This additional dataset was also created using synthetic data from GNU Radio. Three datasets were created with varying input size (128, 256, and 512). These synthetic datasets consists of 5 modulation schemes: BPSK, QPSK, 8PSK, QAM16, and QAM64. Keeping with the RML2016.10A Dataset, the samples per symbol of the root raised cosine filter were fixed at 8. The one sided filter span in symbols is varied uniformly from 7 to 10 with a step size of 1. The roll-off factor of the root raised cosine was varied uniformly from 0.34 to 0.36 with a step size of 0.01. For the channel model, the modulated signal was subjected to AWGN and given a center frequency offset as described by (10) to simulate errors in the receiver's signal detection stage [33]. The power of the AWGN is calculated using E_s/N_o and varied uniformly from 0 dB to 20 dB with a step size of 2. The center frequency offset, which was normalized to the sample rate, is swept uniformly from -1% to 1% with a step size of 0.2%.

4) Training Results: The network is implemented in PyTorch and trained using an NVIDIA 1080 GPU with the Adam [32] optimizer. The batch size used is 1024 when the network is trained with Dataset A and 512 when trained with Dataset B due to the increased example sizes. Models trained on Dataset A use dropout for regularization, as was initially proposed in [8]; however, models trained on Dataset B use Batch Normalization as this increased training stability for the larger example sizes. For all models, the learning rate is set to 0.001 and early stopping is employed with a patience of 5.

During training, 30% of the dataset was withheld as a test set. The remaining 70% of the data is used in the training sequence with 5% of the training set used as a validation set. All data is split randomly with the exception that modulation classes and SNR are kept balanced for all sets. Each of the models is then evaluated at each SNR in the test set for overall accuracy and the results are shown in Figure 4. As expected, increasing the input size lead to increasing accuracy.
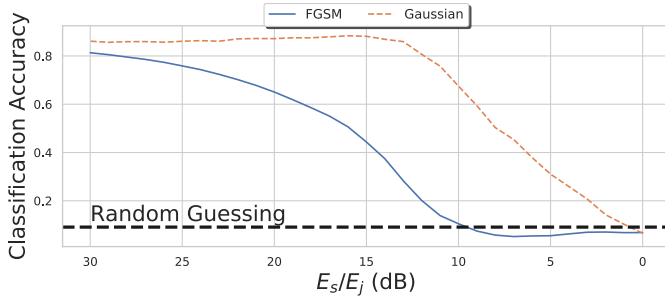
Fig. 5. Overall classification accuracy of a model trained on Dataset A for a direct access attack. This plot compares the classification accuracy when FGSM in used to apply a specific adversarial perturbation to the accuracy when "jammed" with a Gaussian noise signal at the same power ratio.
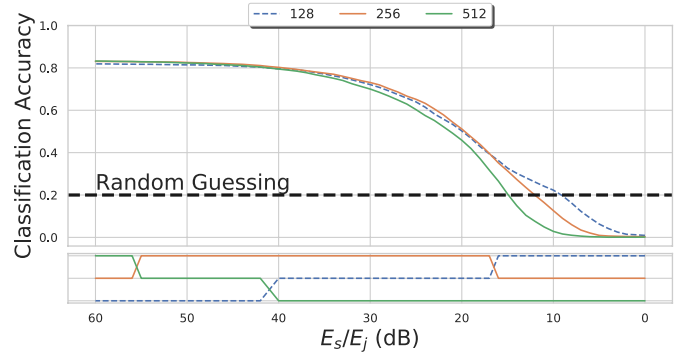

Fig. 6. Overall classification accuracy (top) of models trained on Dataset B in the presence of a direct access FGSM attack. The relative classification accuracy ranking of the three different models for each E_s/E_j (bottom).

V. ANALYSIS OF DIRECT ACCESS ATTACKS

In order to first characterize the effectiveness of adversarial machine learning on raw-IQ based AMC, a baseline study of average classification accuracy against E_s/E_j was performed using the model trained on Dataset A. This attack was performed with no noise added to the adversarial examples and thus assumes direct access to the classifier input.

As can be seen in Figure 5, even at 30 dB, the FGSM attack is more effective than simply adding Gaussian noise (AWGN). At 10 dB, the FGSM attack is effective enough to degrade the classifier below the performance of random guessing. This represents an 8 dB improvement over the same degradation using Gaussian noise.

For comparison to other results in CV literature, we can plug $E_s/E_j = 10$ dB into (8) which yields that an ϵ of ≈ 0.079 is sufficient for accomplishing the goal of untargeted adversarial machine learning for direct access attacks on this model. While this clearly shows an improvement over Gaussian jamming, this perturbation is larger than the original example shown in [19] of 0.007 for performing an untargeted attack using a source image of a panda. However, that result used ImageNet as a source class and GoogLeNet [34] as the model where the input dimensions of the image were at least $3 \times 256 \times 256$ ($\gg \mathbb{R}^{196,608}$) while the input size considered here is $1 \times 2 \times 128$ ($\mathbb{R}^{256}$). Therefore, while we know that the underlying classification task is vastly different and exact perturbation constraints cannot be directly compared, we next investigate whether increased input dimensionality makes the model more susceptible to adversarial examples.

A. Attack Effectiveness versus NN Input Size

Increasing the DNN input size has been empirically shown to improve the performance of raw-IQ AMC in [33] as well as the current work's reproduction of similar results in Figure 4. While it is intuitive that viewing longer time windows of a signal will allow for higher classification accuracy, it is also intuitive that allowing more adversarial jamming energy to enter the algorithm will have adverse effects. Therefore, the current work presents an experiment used to verify this intuition. Three copies of the same network, that differ only

in input size, are trained on Dataset B. The analysis from the previous section is then repeated and shown in Figure 6.

As expected, at very high E_s/E_j, where the adversarial energy is low, the network with the largest input size is the most accurate. However, it is quickly supplanted by the second largest input size when E_s/E_j drops below 55 dB ($\epsilon \approx 0.00044$). Once E_s/E_j drops below 15 dB, the classification accuracy ranking inverts from the initial rankings, with the smallest input size being the most accurate and the largest input size being the least accurate. Therefore, when developing a RFML system for use in adversarial environments, the benefits of increasing input size must be balanced against the cost of increasing the attack surface.

B. Analyzing Individual Adversarial Examples

While the earlier subsections presented macro-level results, this subsection presents results at a micro-level by analyzing the fine grained effect of the adversarial machine learning method on individual examples rather than the average effect across multiple examples. The current work considers a single machine learning example from each of the source modulations[4]. For each example, E_s/E_j is swept from 40 to 0 dB with a step size of a 1 dB. At each E_s/E_j, the outputs of the DNN before the softmax function (as was shown in [19]) are captured.

One adversarial example for BPSK is shown in Figure 2. It can be seen in the Q samples that, due to the sign operation in (9), the perturbation applied to the signal has a box shape. Therefore, the perturbation alone is easily identifiable; however, in the I samples, where the underlying modulated signal also lies, it is less distinguishable. Notably, the differences are most apparent around the symbol locations (note that this signal has 8 samples per symbol), which could indicate that the classifier has learned some notion of synchronization.

1) Difference in Logits: While the full output of the DNN provides ample information, it is multi-dimensional and therefore hard to visualize. One metric that is often used is a confusion matrix, which captures the relationships among classes. However, confusion matrices are generally

[4]While random individual examples are analyzed for simplicity, the conclusions drawn are further explored in Section VI.
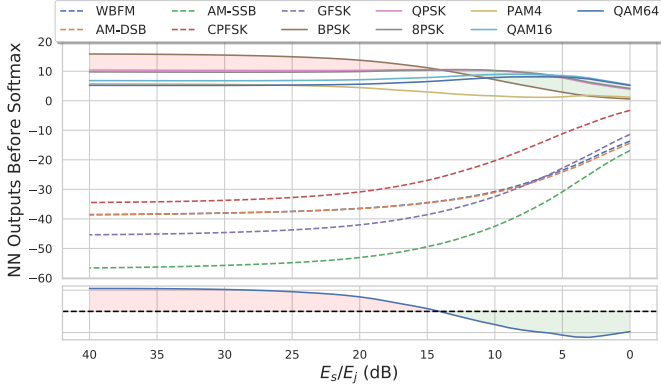
Fig. 7. Output of the model trained on Dataset A for a direct access FGSM attack using a single BPSK adversarial example across varying E_s/E_j (top) and the corresponding difference in logits (bottom).

Fig. 8. Output of the model trained on Dataset A for a direct access FGSM attack using a single QAM16 adversarial example across varying E_s/E_j (top) and the corresponding difference in logits (bottom)

only presented as an average across multiple examples and do not provide any notion of the confidence with which a classifier made the prediction. Therefore, a confusion matrix would not fully capture the variance of the DNN because the outputs would not change unless the input examples were moved across a decision boundary. Another metric that could be used is to apply the softmax function to the output and report the confidence associated with the source class. This metric shows the variance of the classifier output but does not provide any indication of the Top-1 accuracy score because even a low confidence output could still be the highest and therefore the predicted class.

The current work presents an additional metric, which we term the "difference in logits" (Δ_{logits}), that simultaneously captures the accuracy of the classifier as well as the variance in outputs. "Logits" refers to the DNN output before the softmax function has been applied. The maximum output of all incorrect classes is subtracted from the source (true) class output, which can be described by the following Equation.

$$\Delta_{logits} = y_s - \max(y_i \forall i \neq s) \qquad (11)$$

The difference in logits can be visualized as the shaded region in the top of Figures 7 and 8. When Δ_{logits} is positive, the example is correctly classified and a negative Δ_{logits} therefore indicates untargeted adversarial success.

2) Classifier Output versus E_s/E_j: The output of the classifier for the BPSK example, across multiple E_s/E_j is shown in Figure 7. At an E_s/E_j of 10 dB, the jamming intensity present in Figure 2, untargeted misclassification is achieved because the BPSK output is not the highest output of the classifier; this result is also indicated by viewing that Δ_{logits} is negative. However, even though misclassification is achieved, the signal is still classified as a linearly modulated signal, with the predicted modulation order increasing as E_s/E_j increased. Linearly modulated signals have symbols which exist in the IQ plane (distinguished as solid lines in Figure 7) versus a FSK or continuous signal (distinguished as dashed lines) whose symbols exist in the frequency domain or do not have discrete symbols at all, respectively. Therefore, while the adversarial machine learning method was able to
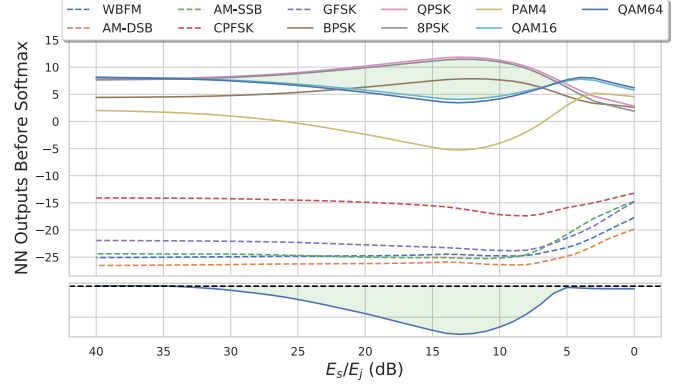
achieve untargeted misclassification by causing the classifier to misinterpret the specific linearly modulated signal, the classifier still captured the hierarchical family of the human-engineered modulation. This reinforces the natural notion that the difficulty of targeted adversarial machine learning varies based on the specific source and target modulations used.

Figure 8 shows the output of the classifier for a single QAM16 example. As was observed in Figure 7, at very low E_s/E_j, where the attack intensity is the highest, the example is again classified as QAM (though untargeted misclassification is narrowly achieved because the model believes it is QAM64). Further, the QAM16 example required much lower energy ($E_s/E_j < 30$ dB) than the BPSK example ($E_s/E_j < 15$ dB) to achieve untargeted misclassification. Therefore, increasing the perturbation energy does not always provide advantageous effects from the evasion perspective, as can be observed from the difference in logits of Figure 8, and the optimal attack intensity varies between source modulations.

3) Mutation Testing with AWGN: Mutation testing was proposed as a defense in [35] where the authors repeatedly applied domain specific noise to a machine learning example and calculated the input's sensitivity, with respect to the classifier output, in the presence of this noise. The authors of [35] found that adversarial examples were more sensitive to noise than examples contained in the initial training distribution and therefore mutation testing could be used to detect adversarial examples.

The current work presents a study of the effect of AWGN, one of the most prevalent models of noise in RFML, on individual adversarial examples. For each E_s/E_j, AWGN is introduced to the signal at varying E_s/N_0 (SNR). E_s/N_0 is swept from 20 to 0 dB with a step size of 1 dB. For each of the SNRs considered, 1000 trials are performed. While E_s/E_j and E_s/N_0 are the parameters swept in this experiment, the jamming to noise ratio (E_j/N_0) can be quickly inferred by

$$\begin{aligned} \frac{E_j}{N_0} &= \frac{E_s/N_0}{E_s/E_j} \\ &= \frac{E_s}{N_0}\text{dB} - \frac{E_s}{E_j}\text{dB} \end{aligned} \qquad (12)$$
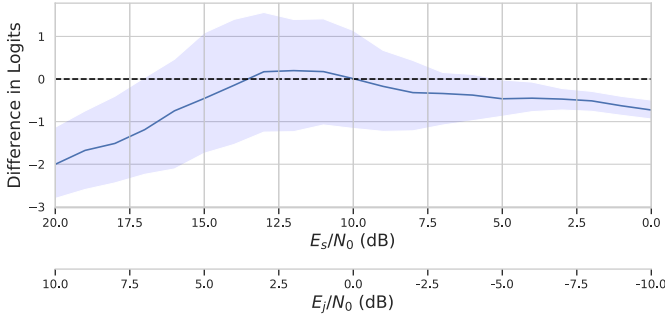
Fig. 9. The effect of noise on the output of the model trained on Dataset A for a single BPSK adversarial example with an E_s/E_j of 10 dB. The line represents the mean of the difference in logits, at a specific E_s/N_0, while the shaded region represents the 25th and 75th percentiles.

Fig. 10. The effect of noise on the output of the model trained on Dataset A for a single QPSK adversarial example with an E_s/E_j of 10 dB. The line represents the mean of the difference in logits, at a specific E_s/N_0, while the shaded region represents the 25th and 75th percentiles.

Again, results are presented in Figure 9 from the BPSK example originally shown in Figure 2, where E_s/E_j is 10 dB. The mean of the difference in logits is shown with the 25th and 75th percentiles shaded to show the variance in the output of the classifier at each SNR. With even a small amount of noise (E_s/N_0 of 17 dB) the 75th percentile of the difference in logits becomes positive indicating that the example was classified correctly in some iterations. Increasing the noise power to roughly half that of the applied perturbation (E_j/N_0 of 3 dB) results in the classification, on average, being correct.

This effect was not observed across all adversarial examples tested. In Figure 10 it is shown that, while the increased sensitivity of the classifier output is observed in the same range of E_j/N_0, it does not result in a correct classification. Therefore, while [35] presented general conclusions that all adversarial examples were sensitive to noise, these results show that this effect is most pronounced when the adversarial perturbation and noise have similar power. Additionally, these effects were not observed at all in the individual 8PSK and QAM16 examples studied.

This section has shown a baseline result that deep learning based raw-IQ automatic modulation classification is vulnerable to untargeted adversarial examples. Further, it was shown that although increasing the neural network input size can improve accuracy in non-adversarial scenarios, it can make a classifier more susceptible to deception for a given E_s/E_j. This section also showed that noise can have a negative impact on adversarial success. Therefore, attacks which can only provide a stochastic input to the classifier (self protect) must be evaluated differently than attacks that are able to provide a deterministic input to the classifier (direct access) and thus the following section presents a more detailed study of self protect attacks using the same adversarial machine learning method.

VI. ANALYSIS OF SELF PROTECT ATTACKS

All OTA attacks must consider the impact of receiver effects on adversarial success; furthermore, self protect attacks must balance the secondary goal of evading an adversary with the primary goal of transmitting information across a wireless channel. Neither of these effects have been considered in prior work and therefore, while the previous section studied
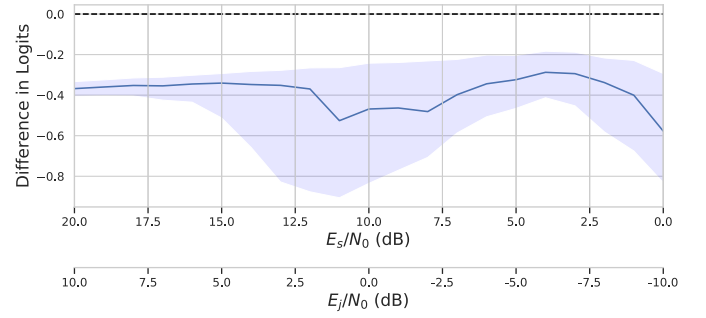
adversarial success in near perfect conditions, this section studies the impact to adversarial success when the examples are evaluated in the presence of three specific receiver effects, which would likely occur during an OTA attack: AWGN, sample time offsets, and center frequency offsets.

A. Additive White Gaussian Noise

AWGN has been shown to negatively impact both BER and classification accuracy. Additionally, as discussed in Section V-B3, AWGN can have a negative effect on adversarial success. This section further evaluates these negative effects with a larger scale study. In some cases, such as in "rubbish examples" [19] or "fooling images" [30], the primary goal of adversarial machine learning may simply be to create an input that is classified with high confidence as some target class starting from a noise input. However, in general, fooling a classifier is a secondary goal that must be balanced against the primary objective. In CV, this primary objective is to preserve human perception of the image. In the current work, the primary objective of self protect attacks is to transmit information to a friendly receiver using a known modulation while the secondary objective is to avoid recognition of that modulation scheme by an eavesdropper. Therefore, this section presents results showing the compounding impacts of adversarial machine learning and AWGN on BER as well as the effect of AWGN on adversarial success rates.

Using the model trained on Dataset A, a range of E_s/N_0 and E_s/E_j are considered. For each E_s/N_0 considered, ten thousand trials are executed to provide averaging of the random variables present in the channel model for a given random signal. The current work considers both the BER and classification accuracy for BPSK in Figure 11 and 8PSK in Figure 12.

Unsurprisingly, increasing the adversarial perturbation energy has positive effects on adversarial success rates (also shown previously in Section V) and negative effects on BER. In order to directly compare the trade space between the two across a range of SNRs, BER versus classification accuracy is plotted for each E_s/E_j considered. At high SNR, extremely low probabilities of bit error, such as those seen in BPSK at $E_s/N_0 = 20$ dB, are hard to characterize empirically. Therefore, in the BER versus classification accuracy plots,
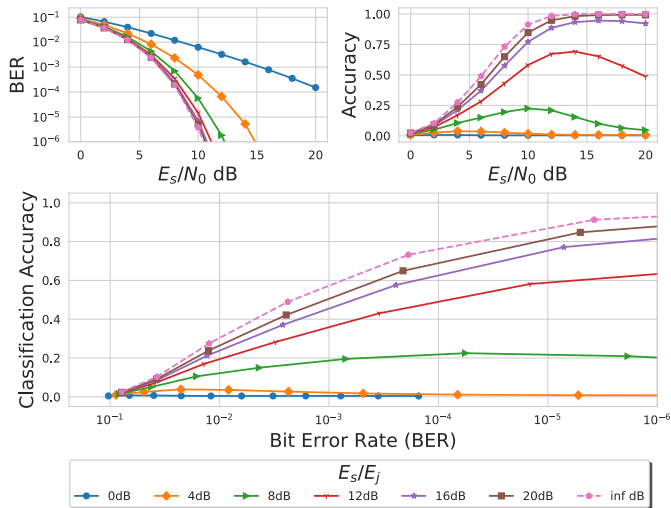
Fig. 11. Classification accuracy and bit error rates at varying E_s/E_j and E_s/N_0 for self protect untargeted adversarial attacks using FGSM on the model trained with Dataset A and a source modulation class of BPSK.

Fig. 12. Classification accuracy and bit error rates at varying E_s/E_j and E_s/N_0 for self protect untargeted adversarial attacks using FGSM on the model trained with Dataset A and a source modulation class of 8PSK.

all results with lower than 10^{-6} BER have been omitted for clarity.

By looking at Figure 11, one can observe that classification accuracy can be degraded to $\approx 0\%$ with no noticeable effect to BER for BPSK when using a white-box adversarial attack with an E_s/E_j of 4 dB. While this is a very strong result, it only occurs at high SNRs (> 15 dB). A more reasonable result to compare to would be the baseline result at 10 dB. In order to achieve the same bit error rate as the baseline of no attack (shown as a dashed line), an adversary must increase their SNR, and therefore their transmission power, by ≈ 2 dB when performing an adversarial attack at an E_s/E_j of 8 dB. A similar analysis can be performed for QPSK where a 4 dB increase to SNR is required to maintain the same BER while reducing classification accuracy to $< 20\%$.

As stated in Section V-B, AWGN can have negative affects on adversarial success. Therefore, while an eavesdropper with a high SNR would be fooled nearly all of the time by a BPSK transmission with an E_s/E_j of 8 dB, an eavesdropper with an E_s/N_0 of 10 dB would still classify this signal correctly 20% of the time. If an adversary wished to attain 0% classification more generally for BPSK using FGSM, then they would need to transmit with an E_s/E_j of 4 dB. This attack intensity would require an SNR increase of ≈ 4 dB to maintain the same BER. The increased accuracy, at lower SNRs, observed previously in Figure 7 can also be observed in Figure 11 and therefore generalizes across BPSK examples. This effect can also be observed, to a lesser extent, in the results of 8PSK (Figure 12). Additional experiments showed that the effect is not observed for QPSK or QAM16. Note that Figure 10 previously showed that the increased sensitivity to noise for that QPSK example did not result in crossing the decision boundary. The effect of increased accuracy cannot be concluded from QAM16 results because the baseline results already show a slight accuracy improvement at SNRs around 10 dB.

Evaluating attacker success in the case of higher order modulations such as 8PSK and QAM16 is less clear. Attacks
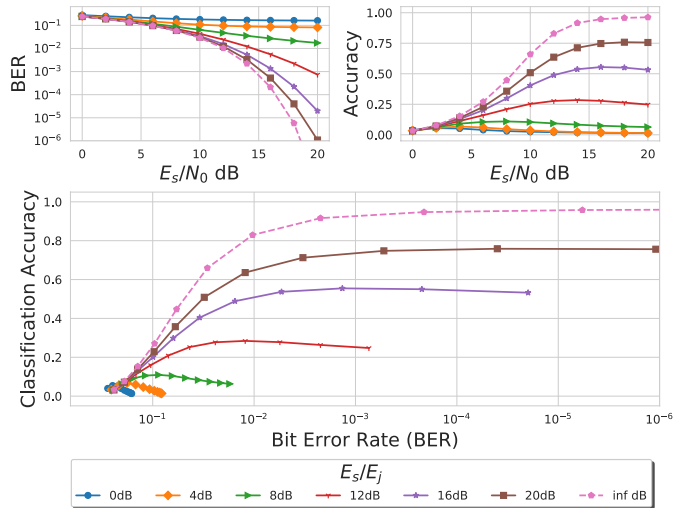
with $E_s/E_j \leq 8$ dB already contain bit errors without any added noise. Therefore, degrading classification accuracy of 8PSK below 20%, outside of the eavesdropper receiving the signal at low SNR, would require forward error correction to account for the errors in transmission. In the case of QAM16, attacks using $E_s/E_j \leq 4$ dB would impact the receiver more than the eavesdropper in many scenarios. Specifically, QAM16 has a BER of $\approx 16\%$ and $\approx 25\%$ when E_s/E_j is 4 and 0 dB respectively even when there is no additive noise. Additionally, note that both of these attack intensities are outside of the optimal range observed in Figure 8. Therefore, when evaluated as a function of BER, the classification accuracy is actually lower in the baseline case than under the presence of these high intensity attacks.

In the case of QAM16, lower intensity attacks are effective at high SNR; however, they become less effective as SNR decreases, an anomalous effect previously discussed in Section V-B. Therefore, untargeted adversarial machine learning with QAM16 as the source modulation class may be most effective in situations where the eavesdropper is thought to have a high fidelity capture of the transmission, such as when the eavesdropper and transmitter are located in close proximity. When the eavesdropper would likely already have a weak view of the signal, it may be more effective to use physical layer security concepts, such as lower transmission power or beam steering, to further degrade the eavesdropper's signal capture.

These results conclude that adversarial machine learning is effective across multiple modulations and SNRs to achieve the goal of untargeted misclassification because, for a given BER, classification can be greatly reduced in many scenarios. However, avoiding signal classification may require sacrificing spectral efficiency or increasing transmission power to maintain the same bit error rate. Additionally, AWGN was shown to have a negative impact on adversarial success rates in 3 out of 4 source modulations tested and therefore adversarial machine learning can be the most effective at high SNRs.
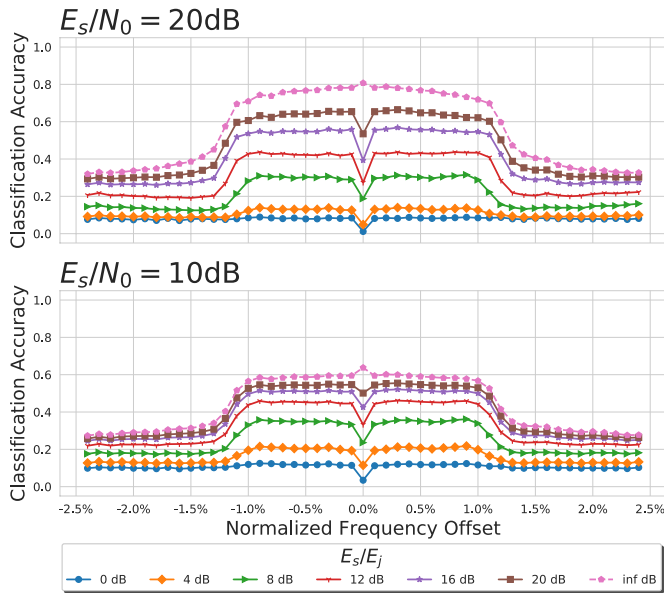
Fig. 13. Classification accuracy vs normalized center frequency offset at varying E_s/E_j for self protect untargeted adversarial attacks using FGSM. The model used is trained on Dataset B with an input size of 128. This dataset has training distribution of $\pm 1\%$ frequency offset that has been normalized to the sample rate.

Fig. 14. Classification accuracy vs time window offsets at varying E_s/E_j for self protect untargeted adversarial attacks using FGSM. The model used is trained on Dataset A.

B. Frequency Offset

Signal classification systems typically do not know when and where a transmission will occur. Therefore, they must take in a wideband signal, detect the frequency bins of the signals present, as well as the start and stop times of transmission, and bring those signals down to baseband for further classification. However, this process is not without error. One effect shown in [33] was the consequences of errors in center frequency estimation, resulting in frequency offset signals. The authors of [33] found that raw-IQ based AMC only generalized over the training distribution it was provided and therefore if additional frequency offsets outside of the training distribution were encountered, the classification accuracy would suffer. Because these estimations are never exact, adversarial examples transmitted over the air must also generalize over these effects.

In order to evaluate the impact of center frequency offsets to adversarial examples, it is necessary to use a model that has been trained to generalize over these effects. Therefore, this experiment uses Dataset B, which has a training distribution consisting of $\pm 1\%$ frequency offsets, which have been normalized to the sample rate. An input size of 128 is used for closer comparison to other results using Dataset A, which only has 128 as an input size. The frequency offsets are swept between -2.5% and 2.5% with a step size of 0.1%. E_s/N_0 is evaluated at 10 and 20 dB. At each SNR, 100 trials are performed to average out the effects of the stochastic process. The results of this experiment are shown in Figure 13.

It can be observed that the baseline classifier has learned to generalize over the effects of frequency offsets within its training range of $\pm 1\%$; however, the adversarial examples are classified with $\approx 10\%$ higher accuracy even at the lowest
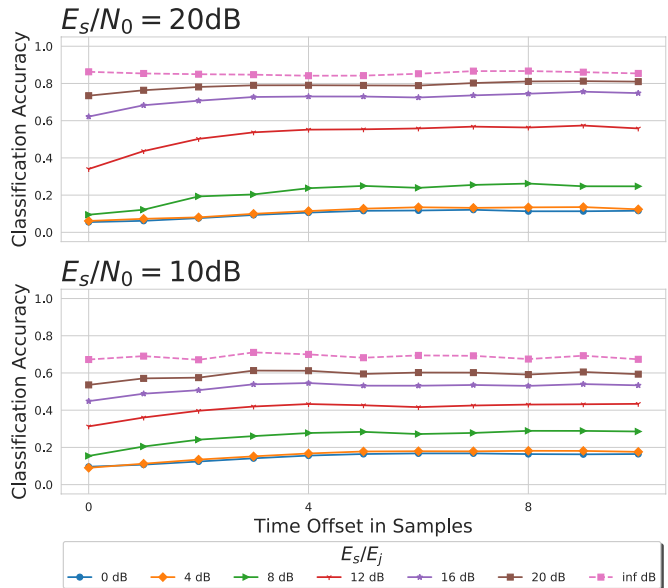
evaluated frequency offsets of $\pm 0.1\%$. This effect is observed at both 20 and 10 dB SNR. Therefore, even minute errors in frequency offset estimation can have negative effects on adversarial machine learning and must be considered by adversarial generation methods.

C. Time Offset

An additional effect that could be encountered is sample time offsets. In the context of communications, sample time offsets can be thought of as a rectangular windowing function, used for creating discrete machine learning examples, not aligning between the adversarial perturbation crafting and signal classification. As previously mentioned, the signal classification system must estimate the start and stop times of a transmission; one way to estimate these times is to use an energy detection algorithm where the power of a frequency range is integrated over time and then thresholded to provide a binary indication of whether a signal is present. A low threshold could have a high false alarm rate and a high threshold could induce a lag in the estimation of the start time. Furthermore, signal classification systems could use overlapping windows for subsequent classifications to increase accuracy through the averaging of multiple classifications of different "views" of a signal or use non-consecutive windows due to real-time computation constraints. Therefore, this effect is a near certainty.

This experiment uses the model trained on Dataset A and again evaluates the effect at an E_s/N_0 of 10 and 20 dB. At each SNR, 100 trials are performed. The time offset is modeled as a shift in the starting index used when slicing the signal for evaluating the signal classification performance and non-overlapping/consecutive windows are still used. The time offset was swept from 0 to 127 (because the input size is 128 and this effect is periodic in the input size); however, only the

results from 0 to 10 are shown for simplicity. Time offsets higher than 8 samples, the symbol period, did not present any significant additional impairments beyond those seen at 8. The results are shown in Figure 14.

As expected, the network is not heavily effected in the baseline case. However, the adversarial examples can be significantly impacted. In the case of an E_s/E_j of 12dB, simply shifting the time window to the right by four samples can increase the classification accuracy by 20%. While some adversarial perturbations have been shown to be agnostic to these time shifts, such as the UAP [23] attack considered in [15], all evaluations of adversarial machine learning in the context of RFML, that seek to model OTA attacks, must assume this effect exists and generalize over it.

VII. Conclusions and Future Work

The current work has demonstrated the vulnerabilities of RFML systems to adversarial examples by evaluating multiple example attacks against a raw-IQ deep learning based modulation classifier. First, it was shown that FGSM [19] crafted perturbations were vastly more effective than perturbations that were crafted using Gaussian noise at degrading the classifier accuracy when the attack was launched with direct access to the classifier input. Furthermore, the current work demonstrated that these vulnerabilities were also present in FGSM based OTA attacks by evaluating the attack effectiveness in the presence of three RFML domain specific receiver effects: AWGN, sample time offsets, and center frequency offsets. When evaluating OTA attacks, evading an eavesdropper is generally a secondary goal and must be balanced against the primary goal of transmission, which is to communicate information across a wireless channel. Therefore, the current work showed that these attacks harmed the eavesdropper more than the adversary by demonstrating that, for a given BER, classification accuracy could be lowered for the majority of the OTA attacks considered. Given these results, it is logical to conclude that similar vulnerabilities exist in all RFML systems when the adversary has white-box knowledge of the classifier.

Future RFML systems must consider these vulnerabilities and develop defenses against them. The current work has shown that, while increasing the number of samples used per classification can increase accuracy in the presence of AWGN, it can also make the model more susceptible to adversarial examples. Therefore, future RFML systems could consider shrinking the input size at the cost of accuracy in the baseline case. Furthermore, the current work has reinforced the viability of mutation testing [35] by showing that RFML domain specific receiver effects typically has a negative impact on adversarial examples. Consequently, using classifications from multiple views of the signal, with different sample time offsets and center frequency offsets, can aid in detecting adversarial examples and even properly classifying them. However, RFML systems are typically SWaP constrained and therefore increasing the number of inferences per time step could limit the bandwidth that can be sensed in real time. Alternatively, defenses could be incorporated into the DNN training phase, which is typically performed offline and thus

has more computational resources or no real-time processing constraint. Ensemble adversarial training [36] has been shown as an effective method for hardening DNN models in the CV domain and the results presented in the current work on BER penalties for adversarial examples can be used to guide which examples to include during training. RFML does not necessarily need to classify all adversarial examples properly, but, it could seek to balance an adversary's increasing success in evading the eavesdropper versus their degrading ability to communicate information.

Future OTA adversarial evasion attacks must consider their ability to generalize over RFML domain specific receiver effects as well as their their impact to the underlying transmission. The current work has demonstrated that all three receiver effects considered can degrade the adversary's ability to evade classification. Furthermore, the current work has shown that, while current adversarial methodology can be used for evading classification, especially when using a lower order source modulation such as BPSK, it may require sacrificing spectral efficiency or increasing transmission power to maintain the same bit error rate. Preliminary efforts in presenting additional adversarial methodology may simply evaluate these effects, as we have done in this current work. However, more advanced efforts may directly incorporate these models of receiver effects and wireless communications goals directly into their adversarial methodology in order to create strong adversarial examples that generalize over receiver effects and have limited impact to the underlying transmission.

The current work concludes that adversarial machine learning is a credible and evolving threat to RFML systems that must be considered in future research.

References

[1] S. M. Dudley, W. C. Headley, M. Lichtman, E. Y. Imana, X. Ma, M. Abdelbar, A. Padaki, A. Ullah, M. M. Sohul, T. Yang, and J. H. Reed, "Practical issues for spectrum management with cognitive radios," *Proc. of the IEEE*, vol. 102, no. 3, pp. 242–264, 2014.

[2] O. A. Dobre, A. Abdi, Y. Bar-Ness, and W. Su, "Survey of automatic modulation classification techniques: classical approaches and new trends," *IET Commun.*, vol. 1, no. 2, pp. 137–156, 2007.

[3] W. C. Headley, J. D. Reed, and C. R. C. M. d. Silva, "Distributed cyclic spectrum feature-based modulation classification," in *IEEE Wireless Commun. and Netw. Conf.*, pp. 1200–1204, 2008.

[4] D. T. Kawamoto and R. W. McGwier, "Rigorous moment-based automatic modulation classification," *Proc. of the GNU Radio Conf.*, vol. 1, no. 1, 2016.

[5] A. Hazza, M. Shoaib, S. A. Alshebeili, and A. Fahad, "An overview of feature-based methods for digital modulation classification," in *1st Int. Conf. on Commun., Signal Proc., and their App.*, pp. 1–6, 2013.

[6] M. M. T. Abdelreheem and M. O. Helmi, "Digital modulation classification through time and frequency domain features using neural networks," in *2012 IX Int. Sym. on Telecommun.*, pp. 1–5, 2012.

[7] M. Bari, A. Khawar, M. Doroslovaki, and T. C. Clancy, "Recognizing fm, bpsk and 16-qam using supervised and unsupervised learning techniques," in *49th Asilomar Conf. on Signals, Systems and Computers*, pp. 160–163, 2015.

[8] T. J. OShea, J. Corgan, and T. C. Clancy, "Convolutional radio modulation recognition networks," in *Int. conf. on engineering app. of neural networks*, pp. 213–226, Springer, 2016.

[9] N. E. West and T. O'Shea, "Deep architectures for modulation recognition," in *IEEE Int. Symposium on Dynamic Spectrum Access Networks (DySPAN)*, pp. 1–6, IEEE, 2017.

[10] K. Karra, S. Kuzdeba, and J. Petersen, "Modulation recognition using hierarchical deep neural networks," in *IEEE Int. Symposium on Dynamic Spectrum Access Networks (DySPAN)*, pp. 1–3, 2017.

[11] J. L. Ziegler, R. T. Arn, and W. Chambers, "Modulation recognition with gnu radio, keras, and hackrf," in *IEEE Int. Symposium on Dynamic Spectrum Access Networks (DySPAN)*, pp. 1–3, 2017.

[12] T. OShea and J. Hoydis, "An introduction to deep learning for the physical layer," *IEEE Transactions on Cognitive Commun. and Netw.*, vol. 3, no. 4, pp. 563–575, 2017.

[13] L. J. Wong, W. C. Headley, S. Andrews, R. M. Gerdes, and A. J. Michaels, "Clustering learned cnn features from raw i/q data for emitter identification," in *IEEE Military Commun. Conf. (MILCOM)*, 2018.

[14] L. Huang, A. D. Joseph, B. Nelson, B. I. Rubinstein, and J. D. Tygar, "Adversarial machine learning," in *Proc. of the 4th ACM Workshop on Security and Artificial Intelligence*, AISec '11, (New York, NY, USA), pp. 43–58, ACM, 2011.

[15] M. Sadeghi and E. G. Larsson, "Adversarial attacks on deep-learning based radio signal classification," *IEEE Wireless Commun. Letters*, pp. 1–1, 2018.

[16] Y. Shi, Y. E. Sagduyu, T. Erpek, K. Davaslioglu, Z. Lu, and J. H. Li, "Adversarial deep learning for cognitive radio security: Jamming attack and defense strategies," in *IEEE Int. Conf., on Commun. Workshops (ICC Workshops)*, pp. 1–6, 2018.

[17] R. Chen, J.-M. Park, and J. Reed, "Defense against primary user emulation attacks in cognitive radio networks," *IEEE Journal on Selected Areas in Commun.*, vol. 26, no. 1, pp. 25–37, 2008.

[18] K. I. Talbot, P. R. Duley, and M. H. Hyatt, "Specific emitter identification and verification," *Technology Review*, vol. 113, 2003.

[19] I. Goodfellow, J. Shlens, and C. Szegedy, "Explaining and harnessing adversarial examples," in *Int. Conf. on Learning Representations*, 2015.

[20] N. Papernot, P. McDaniel, S. Jha, M. Fredrikson, Z. B. Celik, and A. Swami, "The limitations of deep learning in adversarial settings," in *IEEE European Symposium on Security and Privacy (EuroS&P)*, pp. 372–387, IEEE, 2016.

[21] Y. Liu, S. Ma, Y. Aafer, W.-C. Lee, J. Zhai, W. Wang, and X. Zhang, "Trojaning attack on neural networks," in *25nd Annual Network and Distributed System Security Symposium, NDSS 2018, San Diego, California, USA, February 18-221, 2018*, The Internet Society, 2018.

[22] M. Jagielski, A. Oprea, B. Biggio, C. Liu, C. Nita-Rotaru, and B. Li, "Manipulating machine learning: Poisoning attacks and countermeasures for regression learning," in *IEEE Symposium on Security and Privacy (SP)*, pp. 19–35, 2018.

[23] S.-M. Moosavi-Dezfooli, A. Fawzi, O. Fawzi, and P. Frossard, "Universal adversarial perturbations," *2017 IEEE Conf. on Computer Vision and Pattern Recognition (CVPR)*, pp. 86–94, 2017.

[24] S. Baluja and I. Fischer, "Adversarial transformation networks: Learning to generate adversarial examples," *arXiv:1703.09387*, 2017.

[25] Y. Dong, F. Liao, T. Pang, H. Su, J. Zhu, X. Hu, and J. Li, "Boosting adversarial attacks with momentum," in *Proc. of the IEEE Conf. on Computer Vision and Pattern Recognition*, 2018.

[26] T. Newman and T. Clancy, "Security threats to cognitive radio signal classifiers," in *Virginia Tech Wireless Personal Commun. Symp.*, 2009.

[27] T. C. Clancy and A. Khawar, "Security threats to signal classifiers using self-organizing maps," in *4th Int. Conf. on Cognitive Radio Oriented Wireless Netw. and Commun.*, pp. 1–6, 2009.

[28] Y. Shi, T. Erpek, Y. E. Sagduyu, and J. H. Li, "Spectrum data poisoning with adversarial deep learning.," in *IEEE Military Commun. Conf. (MILCOM)*, 2018.

[29] T. J. O'Shea and N. West, "Radio machine learning dataset generation with gnu radio," in *Proc. of the GNU Radio Conf.*, vol. 1, 2016.

[30] A. Nguyen, J. Yosinski, and J. Clune, "Deep neural networks are easily fooled: High confidence predictions for unrecognizable images," in *Proc. IEEE Conf. on Comp. Vision and Pattern Recog.*, pp. 427–436, 2015.

[31] N. Papernot, P. D. McDaniel, I. J. Goodfellow, S. Jha, Z. B. Celik, and A. Swami, "Practical black-box attacks against machine learning," in *Proc. of the 2017 ACM on Asia Conf. on Computer and Commun. Security, AsiaCCS 2017, Abu Dhabi, United Arab Emirates, April 2-6, 2017*, pp. 506–519, 2017.

[32] D. P. Kingma and J. Ba, "Adam: A method for stochastic optimization," *CoRR*, vol. abs/1412.6980, 2014.

[33] S. C. Hauser, W. C. Headley, and A. J. Michaels, "Signal detection effects on deep neural networks utilizing raw iq for modulation classification," in *Military Commun. Conf.*, pp. 121–127, IEEE, 2017.

[34] C. Szegedy, L. Wei, J. Yangqing, P. Sermanet, S. Reed, D. Anguelov, D. Erhan, V. Vanhoucke, and A. Rabinovich, "Going deeper with convolutions," in *IEEE Conf. on Computer Vision and Pattern Recognition (CVPR)*, pp. 1–9, 2015.

[35] J. Wang, J. Sun, P. Zhang, and X. Wang, "Detecting adversarial samples for deep neural networks through mutation testing," *CoRR*, vol. abs/1805.05010, 2018.

[36] F. Tramèr, A. Kurakin, N. Papernot, D. Boneh, and P. D. McDaniel, "Ensemble adversarial training: Attacks and defenses," *CoRR*, vol. abs/1705.07204, 2017.